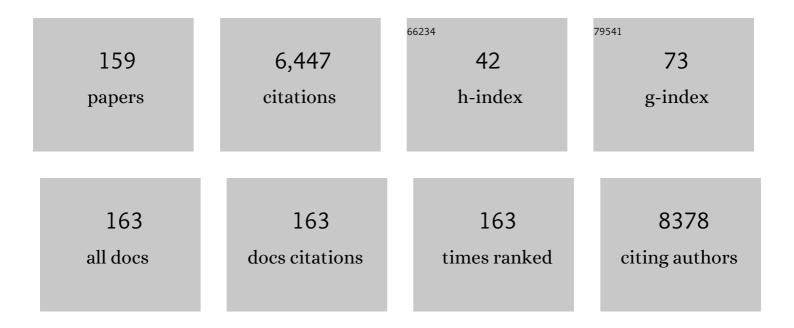
List of Publications by Year in descending order

Source: https://exaly.com/author-pdf/4777824/publications.pdf Version: 2024-02-01



#	Article	IF	CITATIONS
1	A stable biosensor for organophosphorus pesticide detection based on chitosan modified graphene. Biotechnology and Applied Biochemistry, 2022, 69, 567-575.	1.4	12
2	Acetic acid acting as a signaling molecule in the quorum sensing system increases 2,3-butanediol production in <i>Saccharomyces cerevisiae</i> . Preparative Biochemistry and Biotechnology, 2022, 52, 487-497.	1.0	5
3	Propelling the practical application of the intimate coupling of photocatalysis and biodegradation system: System amelioration, environmental influences and analytical strategies. Chemosphere, 2022, 287, 132196.	4.2	15
4	Critical Role of Phosphorus in Hollow Structures Cobaltâ€Based Phosphides as Bifunctional Catalysts for Water Splitting. Small, 2022, 18, e2103561.	5.2	54
5	Dealloyed nanoporous copper as a highly active catalyst in Fenton-like reaction for degradation of organic pollutants. Chemical Engineering Journal, 2022, 431, 133834.	6.6	8
6	Mechanical properties of brain tissue based on microstructure. Journal of the Mechanical Behavior of Biomedical Materials, 2022, 126, 104924.	1.5	9
7	Elaeagnus angustifolia can improve salt-alkali soil and the health level of soil: Emphasizing the driving role of core microbial communities. Journal of Environmental Management, 2022, 305, 114401.	3.8	13
8	Otolith Microstructure Analysis Reveals Different Growth Histories of Japanese Sardine (Sardinops) Tj ETQq0 0 0	rgBT/Over	lock 10 Tf 50

9	Growth and early life stage of Antarctic silverfish (Pleuragramma antarctica) in the Amundsen Sea of the Southern Ocean: evidence for a potential new spawning/nursery ground. Polar Biology, 2022, 45, 359-368.	0.5	2
10	Study on Machine Learning Models for Building Resilience Evaluation in Mountainous Area: A Case Study of Banan District, Chongqing, China. Sensors, 2022, 22, 1163.	2.1	9
11	Lithium Saltâ€Induced In Situ Polymerizations Enable Double Network Polymer Electrolytes. Macromolecular Rapid Communications, 2022, 43, e2100853.	2.0	1
12	Buffer species-dependent catalytic activity of Cu-Adenine as a laccase mimic for constructing sensor array to identify multiple phenols. Analytica Chimica Acta, 2022, 1204, 339725.	2.6	18
13	Tough, Highly Oriented, Super Thermal Insulating Regenerated All-Cellulose Sponge-Aerogel Fibers Integrating a Graded Aligned Nanostructure. Nano Letters, 2022, 22, 3516-3524.	4.5	34
14	Aerobic composting of chicken manure with penicillin G: Community classification and quorum sensing mediating its contribution to humification. Bioresource Technology, 2022, 352, 127097.	4.8	16
15	Modulating anion defect in La0.6Sr0.4Co0.8Fe0.2O3-Î [′] for enhanced catalytic performance on peroxymonosulfate activation: Importance of hydrated electrons and metal-oxygen covalency. Journal of Hazardous Materials, 2022, 432, 128686.	6.5	23
16	High-performance, low-cost nanoporous alloy actuators by one-step dealloying of Al-Ni-Cu precursors. Intermetallics, 2022, 145, 107537.	1.8	4
17	F, N neutralizing effect induced Co-P-O cleaving endows CoP nanosheets with superior HER and OER performances. Journal of Colloid and Interface Science, 2022, 619, 298-306.	5.0	33
18	Highly Stable Grapheneâ€Based Flexible Hybrid Transparent Conductive Electrodes for Organic Solar Cells. Advanced Materials Interfaces, 2022, 9, .	1.9	19

#	Article	IF	CITATIONS
19	Advances in <scp>host selection</scp> and <scp>interface regulation</scp> of polymer electrolytes. Journal of Polymer Science, 2022, 60, 743-765.	2.0	8
20	Exsolution of CoFe(Ru) nanoparticles in Ru-doped (La0.8Sr0.2)0.9Co0.1Fe0.8Ru0.1O3â^î^ for efficient oxygen evolution reaction. Nano Research, 2022, 15, 6977-6986.	5.8	34
21	Structural Engineering of Ultrathin, Lightweight, and Bendable Electrodes Based on a Nanowire Network Current Collector Enables Flexible Energy-Storage Devices. ACS Applied Energy Materials, 2022, 5, 5785-5796.	2.5	2
22	Highly stable, stretchable, and versatile electrodes by coupling of NiCoS nanosheets with metallic networks for flexible electronics. Nanoscale, 2022, 14, 8172-8182.	2.8	5
23	Composite electrodes with NiCoAl-LDH coated Ti3C2Tx MXene and incorporated Ag nanowires for screen-printable in-plane hybrid supercapacitors on textiles. Applied Surface Science, 2022, 598, 153796.	3.1	20
24	CuxO-Modified Nanoporous Cu Foil as a Self-Supporting Electrode for Supercapacitor and Oxygen Evolution Reaction. Nanomaterials, 2022, 12, 2121.	1.9	3
25	Evaluation of catalytic deoxygenation of soluble species from a coal using mass spectrometers. Energy Sources, Part A: Recovery, Utilization and Environmental Effects, 2021, 43, 1363-1372.	1.2	0
26	A Sawtooth MEMS Capacitive Strain Sensor for Passive Telemetry in Bearings. IEEE Sensors Journal, 2021, 21, 22527-22535.	2.4	5
27	Natural bamboo leaves as dielectric layers for flexible capacitive pressure sensors with adjustable sensitivity and a broad detection range. RSC Advances, 2021, 11, 17291-17300.	1.7	15
28	Reusable Ruthenium Microspheres Derived from Chitin for Highly Efficient and Selective Hydroboration of Imines. ACS Sustainable Chemistry and Engineering, 2021, 9, 1568-1575.	3.2	8
29	Nanoporous copper as an inexpensive electrochemical actuator responsive to sub-volt voltages. Electrochemistry Communications, 2021, 124, 106940.	2.3	16
30	Digital Design and Application of 3D Printed Surgical Guide for Long Screw Fixation of Condylar Sagittal Fracture. Journal of Craniofacial Surgery, 2021, 32, e632-e634.	0.3	4
31	Three-dimensional nanoporous tungsten supported tellurium cathode for Li-Te batteries. Journal of Alloys and Compounds, 2021, 861, 158459.	2.8	1
32	Novel oxygen permeable hollow fiber perovskite membrane with surface wrinkles. Separation and Purification Technology, 2021, 261, 118295.	3.9	33
33	Scalable Solution-Processed Fabrication Approach for High-Performance Silver Nanowire/MXene Hybrid Transparent Conductive Films. Nanomaterials, 2021, 11, 1360.	1.9	24
34	Morphological and compositional modification of β-Ni(OH)2 nanoplates by ferrihydrite for enhanced oxygen evolution reaction. International Journal of Hydrogen Energy, 2021, 46, 17720-17730.	3.8	12
35	Tidally Induced Temporal Variations in Growth of Youngâ€ofâ€theâ€Year Pacific Cod in the Yellow Sea. Journal of Geophysical Research: Oceans, 2021, 126, e2020JC016696.	1.0	6
36	Stretchable Strain Sensors Based on Two- and Three-Dimensional Carbonized Cotton Fabrics for the Detection of Full Range of Human Motions. ACS Applied Electronic Materials, 2021, 3, 3287-3295.	2.0	14

#	Article	IF	CITATIONS
37	Formulating a GIS-based geometric design quality assessment model for Mountain highways. Accident Analysis and Prevention, 2021, 157, 106172.	3.0	8
38	Microstructured capacitive sensor with broad detection range and long-term stability for human activity detection. Npj Flexible Electronics, 2021, 5, .	5.1	42
39	Microstructure Engineering of Stretchable Resistive Strain Sensors with Discrimination Capabilities in Transverse and Longitudinal Directions. Macromolecular Materials and Engineering, 2021, 306, 2100283.	1.7	8
40	Dealloying-Derived Nanoporous Cu6Sn5 Alloy as Stable Anode Materials for Lithium-Ion Batteries. Materials, 2021, 14, 4348.	1.3	5
41	Nanoporous silver-modified LaCoO3-δ perovskite for oxygen reduction reaction. Electrochimica Acta, 2021, 391, 138908.	2.6	15
42	Perovskite and related oxide based electrodes for water splitting. Journal of Cleaner Production, 2021, 318, 128544.	4.6	70
43	Electrospun cobalt Prussian blue analogue-derived nanofibers for oxygen reduction reaction and lithium-ion batteries. Journal of Colloid and Interface Science, 2021, 599, 280-290.	5.0	23
44	Large-Scale, Cuttable, Full Tissue-Based Capacitive Pressure Sensor for the Detection of Human Physiological Signals and Pressure Distribution. ACS Omega, 2021, 6, 27208-27215.	1.6	9
45	Stability of SiNx Prepared by Plasma-Enhanced Chemical Vapor Deposition at Low Temperature. Nanomaterials, 2021, 11, 3363.	1.9	4
46	Voltage window-dependent electrochemical performance and reaction mechanisms of Na3V2(PO4)3 cathode for high-capacity sodium ion batteries. Ionics, 2020, 26, 2343-2351.	1.2	20
47	On the dealloying mechanisms of a rapidly solidified Al80Ag20 alloy using in-situ X-ray diffraction. Intermetallics, 2020, 125, 106913.	1.8	4
48	The Driving Risk Analysis and Evaluation in Rightward Zone of Expressway Reconstruction and Extension Engineering. Journal of Advanced Transportation, 2020, 2020, 1-13.	0.9	6
49	Constructed Ag NW@Bi/Al core–shell nano-architectures for high-performance flexible and transparent energy storage device. Nanoscale, 2020, 12, 19308-19316.	2.8	5
50	Transparent and Stretchable Strain Sensors with Improved Sensitivity and Reliability Based on Ag NWs and PEDOT:PSS Patterned Microstructures. Advanced Electronic Materials, 2020, 6, 1901360.	2.6	36
51	NiCo2O4/biomass-derived carbon composites as anode for high-performance lithium ion batteries. Journal of Power Sources, 2020, 451, 227761.	4.0	71
52	Numerical and experimental study of tuned liquid damper effects on suppressing nonlinear vibration of elastic supporting structural platform. Nonlinear Dynamics, 2020, 99, 2675-2691.	2.7	21
53	Binder-Free Nickel Oxide Lamellar Layer Anchored CoOx Nanoparticles on Nickel Foam for Supercapacitor Electrodes. Nanomaterials, 2020, 10, 194.	1.9	6
54	Hybrid Ni(OH) ₂ /FeOOH@NiFe Nanosheet Catalysts toward Highly Efficient Oxygen Evolution Reaction with Ultralong Stability over 1000 Hours. ACS Sustainable Chemistry and Engineering, 2019, 7, 14601-14610.	3.2	39

#	Article	IF	CITATIONS
55	Iron and Nickel Mixed Oxides Derived From NillFell-PBA for Oxygen Evolution Electrocatalysis. Frontiers in Chemistry, 2019, 7, 539.	1.8	22
56	Investigation on the Performance Improvement of Polyacrylonitrile-Derived Flexible Electrospun Carbon Nanofiber Mats. Applied Sciences (Switzerland), 2019, 9, 3683.	1.3	1
57	An integrated high-throughput strategy enables the discovery of multifunctional ionic liquids for sustainable chemical processes. Green Chemistry, 2019, 21, 307-313.	4.6	16
58	Self-supporting, eutectic-like, nanoporous biphase bismuth-tin film for high-performance magnesium storage. Nano Research, 2019, 12, 801-808.	5.8	30
59	Re-evaluation of La0.6Sr0.4Co0.2Fe0.8O3-Ĩ′ hollow fiber membranes for oxygen separation after long-term storage of five and ten years. Journal of Membrane Science, 2019, 587, 117180.	4.1	42
60	Circular RNA circTRIM33–12 acts as the sponge of MicroRNA-191 to suppress hepatocellular carcinoma progression. Molecular Cancer, 2019, 18, 105.	7.9	172
61	Understanding the boosted sodium storage behavior of a nanoporous bismuth-nickel anode using <i>operando</i> X-ray diffraction and density functional theory calculations. Journal of Materials Chemistry A, 2019, 7, 13602-13613.	5.2	20
62	Efficient removal of organic pollutants by ceramic hollow fibre supported composite catalyst. Sustainable Materials and Technologies, 2019, 20, e00108.	1.7	30
63	Hexagonal and Square Patterned Silver Nanowires/PEDOT:PSS Composite Grids by Screen Printing for Uniformly Transparent Heaters. Polymers, 2019, 11, 468.	2.0	33
64	A one-dimensional Ag NW@NiCo/NiCo(OH) ₂ core–shell nanostructured electrode for a flexible and transparent asymmetric supercapacitor. Journal of Materials Chemistry A, 2019, 7, 8184-8193.	5.2	54
65	Decomposition analysis of China's CO2 emissions (2000–2016) and scenario analysis of its carbon intensity targets in 2020 and 2030. Science of the Total Environment, 2019, 668, 432-442.	3.9	128
66	Ternary mesoporous cobalt-iron-nickel oxide efficiently catalyzing oxygen/hydrogen evolution reactions and overall water splitting. Nano Research, 2019, 12, 2281-2287.	5.8	59
67	Mortalin stabilizes CD151-depedent tetraspanin-enriched microdomains and implicates in the progression of hepatocellular carcinoma. Journal of Cancer, 2019, 10, 6199-6206.	1.2	11
68	Transforming Bulk Metals into Metallic Nanostructures: A Liquid-Metal-Assisted Top-Down Dealloying Strategy with Sustainability. ACS Sustainable Chemistry and Engineering, 2019, 7, 3274-3281.	3.2	12
69	Graphitic carbon nitride (g-C3N4)-based photocatalysts for water disinfection and microbial control: A review. Chemosphere, 2019, 214, 462-479.	4.2	304
70	Hierarchically porous Mo-doped Ni–Fe oxide nanowires efficiently catalyzing oxygen/hydrogen evolution reactions. Journal of Materials Chemistry A, 2018, 6, 8430-8440.	5.2	65
71	Hollow and Core–Shell Nanostructure Co ₃ O ₄ Derived from a Metal Formate Framework toward High Catalytic Activity of CO Oxidation. ACS Applied Nano Materials, 2018, 1, 800-806.	2.4	27
72	Metal-free virucidal effects induced by g-C3N4 under visible light irradiation: Statistical analysis and parameter optimization. Chemosphere, 2018, 195, 551-558.	4.2	50

#	Article	IF	CITATIONS
73	A Dealloying Synthetic Strategy for Nanoporous Bismuth–Antimony Anodes for Sodium Ion Batteries. ACS Nano, 2018, 12, 3568-3577.	7.3	167
74	Self-Supported Porous NiSe ₂ Nanowrinkles as Efficient Bifunctional Electrocatalysts for Overall Water Splitting. ACS Sustainable Chemistry and Engineering, 2018, 6, 2231-2239.	3.2	130
75	Transforming bulk alloys into nanoporous lanthanum-based perovskite oxides with high specific surface areas and enhanced electrocatalytic activities. Journal of Materials Chemistry A, 2018, 6, 19979-19988.	5.2	19
76	Circularly Polarized Light Photodetector Based on X-Shaped Chiral Metamaterial. IEEE Sensors Journal, 2018, 18, 9203-9206.	2.4	16
77	Scalable Dealloying Route to Mesoporous Ternary CoNiFe Layered Double Hydroxides for Efficient Oxygen Evolution. ACS Sustainable Chemistry and Engineering, 2018, 6, 16096-16104.	3.2	59
78	Fabrication and characterization of nanoporous Cu–Sn intermetallics <i>via</i> dealloying of ternary Mg–Cu–Sn alloys. CrystEngComm, 2018, 20, 6900-6908.	1.3	8
79	Design and implementation of haptic sensing interface for ankle rehabilitation robotic platform. , 2018, , .		4
80	Visible-light-driven, water-surface-floating antimicrobials developed from graphitic carbon nitride and expanded perlite for water disinfection. Chemosphere, 2018, 208, 84-92.	4.2	64
81	Structure-Designed Synthesis of CoP Microcubes from Metal–Organic Frameworks with Enhanced Supercapacitor Properties. Inorganic Chemistry, 2018, 57, 10287-10294.	1.9	80
82	Time series forecasting based on wavelet decomposition and feature extraction. Neural Computing and Applications, 2017, 28, 183-195.	3.2	6
83	Bundling strategy to simultaneously improve the mechanical strength and oxygen permeation flux of the individual perovskite hollow fiber membranes. Journal of Membrane Science, 2017, 527, 137-142.	4.1	22
84	Design and synthesis of porous ZnTiO ₃ /TiO ₂ nanocages with heterojunctions for enhanced photocatalytic H ₂ production. Journal of Materials Chemistry A, 2017, 5, 11615-11622.	5.2	54
85	N-Doped Graphene from Metal–Organic Frameworks for Catalytic Oxidation of p-Hydroxylbenzoic Acid: N-Functionality and Mechanism. ACS Sustainable Chemistry and Engineering, 2017, 5, 2693-2701.	3.2	243
86	Designing CO ₂ -resistant oxygen-selective mixed ionic–electronic conducting membranes: guidelines, recent advances, and forward directions. Chemical Society Reviews, 2017, 46, 2941-3005.	18.7	164
87	Electrochemical actuation behaviors and mechanisms of bulk nanoporous Ni-Pd alloy. Scripta Materialia, 2017, 137, 73-77.	2.6	22
88	A-Site Excess (La _{0.8} Ca _{0.2}) _{1.01} FeO _{3â^'Î^} (LCF) Perovskite Hollow Fiber Membrane for Oxygen Permeation in CO ₂ -Containing Atmosphere. Energy & Fuels, 2017, 31, 4531-4538.	2,5	23
89	Three-dimensional tetsubo-like Co(OH)2 nanorods on a macroporous electrically conductive network as an efficient electroactive framework for the hydrogen evolution reaction. Journal of Materials Chemistry A, 2017, 5, 2629-2639.	5.2	34
90	An insight into metal organic framework derived N-doped graphene for the oxidative degradation of persistent contaminants: formation mechanism and generation of singlet oxygen from peroxymonosulfate. Environmental Science: Nano, 2017, 4, 315-324.	2.2	372

CHI ZHANG

#	Article	IF	CITATIONS
91	Enhanced oxygen permeability and electronic conductivity of Ce0.8Gd0.2O2â^δ membrane via the addition of sintering aids. Solid State Ionics, 2017, 310, 121-128.	1.3	21
92	Dealloying-directed synthesis of efficient mesoporous CoFe-based catalysts towards the oxygen evolution reaction and overall water splitting. Nanoscale, 2017, 9, 16467-16475.	2.8	67
93	Eutectic-directed self-templating synthesis of PtNi nanoporous nanowires with superior electrocatalytic performance towards the oxygen reduction reaction: experiment and DFT calculation. Journal of Materials Chemistry A, 2017, 5, 23651-23661.	5.2	37
94	Preparation of SnO ₂ Nanoparticles Doped With Palladium and Graphene and Application for Ethanol Detection. IEEE Sensors Journal, 2017, 17, 6240-6245.	2.4	7
95	Selective sampling using active learning for short-term wind speed prediction. , 2017, , .		3
96	Highly efficient field emission from ZnO nanorods and nanographene hybrids on a macroporous electric conductive network. Journal of Materials Chemistry C, 2017, 5, 9296-9305.	2.7	13
97	Solar Photocatalytic Water Oxidation and Purification on ZIF-8-Derived C–N–ZnO Composites. Energy & Fuels, 2017, 31, 2138-2143.	2.5	32
98	Manganese molybdate nanoflakes on silicon microchannel plates as novel nano energetic material. Royal Society Open Science, 2017, 4, 171229.	1.1	5
99	Low-temperature CO oxidation over CeO ₂ and CeO ₂ @Co ₃ O ₄ core–shell microspheres. New Journal of Chemistry, 2017, 41, 13418-13424.	1.4	49
100	UBAP2 negatively regulates the invasion of hepatocellular carcinoma cell by ubiquitinating and degradating Annexin A2. Oncotarget, 2016, 7, 32946-32955.	0.8	22
101	Effect of Ru Species on N2O Decomposition over Ru/Al2O3 Catalysts. Catalysts, 2016, 6, 173.	1.6	21
102	Enhanced CO ₂ Resistance for Robust Oxygen Separation Through Tantalumâ€doped Perovskite Membranes. ChemSusChem, 2016, 9, 505-512.	3.6	22
103	Enhanced Photocatalytic Degradation of 17 <i>α</i> â€Ethinylestradiol Exhibited by Multifunctional ZnFe ₂ O ₄ –Ag/ <scp>rGO</scp> Nanocomposite Under Visible Light. Photochemistry and Photobiology, 2016, 92, 238-246.	1.3	37
104	Photocatalysis of C, N-doped ZnO derived from ZIF-8 for dye degradation and water oxidation. RSC Advances, 2016, 6, 95903-95909.	1.7	79
105	Visible-light-driven photocatalytic inactivation of MS2 by metal-free g-C3N4: Virucidal performance and mechanism. Water Research, 2016, 106, 249-258.	5.3	145
106	Mechanistic study of visible light driven photocatalytic degradation of EDC 17α-ethinyl estradiol and azo dye Acid Black-52: phytotoxicity assessment of intermediates. RSC Advances, 2016, 6, 87246-87257.	1.7	27
107	Nitrogen-doped multilayered nanographene derived from Ni ₃ C with efficient electron field emission. Journal of Materials Chemistry C, 2016, 4, 9251-9260.	2.7	9
108	Enhanced ethanol sensing performance of tin oxide nanoparticles doped with palladium and graphene.		0

7

#	Article	IF	CITATIONS
109	Three-dimensional homo-nanostructured MnO ₂ /nanographene membranes on a macroporous electrically conductive network for high performance supercapacitors. Journal of Materials Chemistry A, 2016, 4, 11317-11329.	5.2	24
110	Catalytic Decomposition of N ₂ O over Co–Ti Oxide Catalysts: Interaction between Co and Ti Oxide. ChemCatChem, 2016, 8, 2155-2164.	1.8	37
111	Analysis of the erythropoietin of a Tibetan Plateau schizothoracine fish (Gymnocypris dobula) reveals enhanced cytoprotection function in hypoxic environments. BMC Evolutionary Biology, 2016, 16, 11.	3.2	44
112	New insight into the difference of PC lipase-catalyzed degradation on poly(butylene succinate)-based copolymers from molecular levels. RSC Advances, 2016, 6, 17896-17905.	1.7	14
113	Enhanced Oxygen Permeation Behavior of Ba _{0.5} Sr _{0.5} Co _{0.8} Fe _{0.2} O _{3â~î^} Membranes in a CO ₂ -Containing Atmosphere with a Sm _{0.2} Ce _{0.8} O _{1.9} Functional Shell. Energy & amp: Fuels. 2016. 30. 1829-1834.	2.5	17
114	Efficient visible light photocatalytic degradation of 17α-ethinyl estradiol by a multifunctional Ag–AgCl/ZnFe ₂ O ₄ magnetic nanocomposite. RSC Advances, 2016, 6, 32761-32769.	1.7	60
115	Preparation of multi-layer graphene on nickel-coated silicon microchannel plates by a hydrothermal carbonization procedure and its improved field emission properties. Journal of Materials Chemistry C, 2016, 4, 2079-2087.	2.7	23
116	Occurrence of endocrine disrupting compounds in aqueous environment and their bacterial degradation: A review. Critical Reviews in Environmental Science and Technology, 2016, 46, 1-59.	6.6	153
117	Generation and characterization of a tetraspanin CD151/integrin α6β1-binding domain competitively binding monoclonal antibody for inhibition of tumor progression in HCC. Oncotarget, 2016, 7, 6314-6322.	0.8	20
118	Conjugating influenza a (H1N1) antigen to nâ€ŧrimethylaminoethylmethacrylate chitosan nanoparticles improves the immunogenicity of the antigen after nasal administration. Journal of Medical Virology, 2015, 87, 1807-1815.	2.5	58
119	Micro <scp>RNA</scp> â€mediated nonâ€cellâ€autonomous regulation of cortical radial glial transformation revealed by a <scp><i>Dicer1</i></scp> knockout mouse model. Glia, 2015, 63, 860-876.	2.5	20
120	Ag@helical chiral TiO2 nanofibers for visible light photocatalytic degradation of 17α-ethinylestradiol. Environmental Science and Pollution Research, 2015, 22, 10444-10451.	2.7	33
121	Hybrid MnO ₂ /C nano-composites on a macroporous electrically conductive network for supercapacitor electrodes. Journal of Materials Chemistry A, 2015, 3, 16695-16707.	5.2	41
122	Hierarchical 3-dimensional CoMoO ₄ nanoflakes on a macroporous electrically conductive network with superior electrochemical performance. Journal of Materials Chemistry A, 2015, 3, 13776-13785.	5.2	61
123	Novel tungsten stabilizing SrCo1â^W O3â^ membranes for oxygen production. Ceramics International, 2015, 41, 14935-14940.	2.3	8
124	Oxygen permeation behavior through Ce _{0.9} Gd _{0.1} O _{2â^îî} membranes electronically short-circuited by dual-phase Ce _{0.9} Gd _{0.1} O _{2â^îî} –Ag decoration. Journal of Materials Chemistry A, 2015, 3, 19033-19041.	5.2	21
125	BRD4 promotes tumor growth and epithelial-mesenchymal transition in hepatocellular carcinoma. International Journal of Immunopathology and Pharmacology, 2015, 28, 36-44.	1.0	49
126	Ce _{0.9} Gd _{0.1} O _{2â^'Î} membranes coated with porous Ba _{0.5} Sr _{0.5} Co _{0.8} Fe _{0.2} O _{3â^´Î} for oxygen separation. RSC Advances, 2015, 5, 5379-5386.	1.7	16

#	Article	IF	CITATIONS
127	Measurement-based performance evaluation of 3D MIMO in high rise scenario. , 2014, , .		4
128	Preparation and evaluation of antigen/N-trimethylaminoethylmethacrylate chitosan conjugates for nasal immunization. Vaccine, 2014, 32, 2582-2590.	1.7	19
129	Unsupported nanoporous Ag catalysts towards CO oxidation. Journal of Molecular Catalysis A, 2014, 382, 55-63.	4.8	29
130	Mercury(ii)-stimulated oxidase mimetic activity of silver nanoparticles as a sensitive and selective mercury(ii) sensor. RSC Advances, 2014, 4, 5867.	1.7	55
131	Ni ₁₂ P ₅ Nanoparticles as an Efficient Catalyst for Hydrogen Generation <i>via</i> Electrolysis and Photoelectrolysis. ACS Nano, 2014, 8, 8121-8129.	7.3	413
132	A new approach to light up the application of semiconductor nanomaterials for photoelectrochemical biosensors: Using self-operating photocathode as a highly selective enzyme sensor. Biosensors and Bioelectronics, 2014, 62, 66-72.	5.3	103
133	Enhanced nitrogen removal and energy saving of intermittent aeration-modified oxidation ditch process. Desalination and Water Treatment, 2014, 52, 4895-4903.	1.0	5
134	In situ formation of p–n junction: A novel principle for photoelectrochemical sensor and its application for mercury(II) ion detection. Analytica Chimica Acta, 2014, 827, 34-39.	2.6	45
135	Comprehensive Multiple Molecular Profile of Epithelial Mesenchymal Transition in Intrahepatic Cholangiocarcinoma Patients. PLoS ONE, 2014, 9, e96860.	1.1	17
136	Correlation analysis of high-speed railway channel parameters based on channel measurement. , 2013, ,		1
137	Ultrafine nanoporous PdFe/Fe3O4 catalysts with doubly enhanced activities towards electro-oxidation of methanol and ethanol in alkaline media. Journal of Materials Chemistry A, 2013, 1, 3620.	5.2	95
138	Adsorption behavior of methyl orange onto nanoporous core–shell Cu@Cu2O nanocomposite. Chemical Engineering Journal, 2013, 223, 76-83.	6.6	78
139	Synthesis of konjac glucomannan phthalate as a new biosorbent for copper ion removal. Journal of Polymer Research, 2013, 20, 1.	1.2	17
140	Synthesis and antibacterial properties of magnetically recyclable nanoporous silver/Fe3O4 nanocomposites through one-step dealloying. CrystEngComm, 2013, 15, 3965.	1.3	19
141	Fabrication of nanoporous Pd with superior hydrogen sensing properties by dealloying. Materials Letters, 2013, 92, 369-371.	1.3	16
142	Solvent-free preparation of polylactic acid fibers by melt electrospinning using umbrella-like spray head and alleviation of problematic thermal degradation. Journal of the Serbian Chemical Society, 2012, 77, 1071-1082.	0.4	30
143	Hitting Time Distributions for Denumerable Birth and Death Processes. Journal of Theoretical Probability, 2012, 25, 950-980.	0.4	22
144	Influence of anion species on electrochemical dealloying of single-phase Al2Au alloy in sodium halide solutions. RSC Advances, 2012, 2, 4481.	1.7	14

#	Article	IF	CITATIONS
145	Dealloying strategy to fabricate ultrafine nanoporous gold-based alloys with high structural stability and tunable magnetic properties. CrystEngComm, 2012, 14, 8292.	1.3	28
146	Tuning the ligament/channel size of nanoporous copper by temperature control. CrystEngComm, 2012, 14, 8352.	1.3	19
147	Ultrafine nanoporous Cu–Pd alloys with superior catalytic activities towards electro-oxidation of methanol and ethanol in alkaline media. RSC Advances, 2012, 2, 11820.	1.7	50
148	Anodization driven enhancement of catalytic activity of Pd towards electro-oxidation of methanol, ethanol and formic acid. Electrochemistry Communications, 2012, 21, 42-45.	2.3	49
149	On the Microstructure, Chemical Composition, and Porosity Evolution of Nanoporous Alloy through Successive Dealloying of Ternary Al–Pd–Au Precursor. Journal of Physical Chemistry C, 2012, 116, 13271-13280.	1.5	44
150	Anodization of Pd in H ₂ SO ₄ Solutions: Influence of Potential, Polarization Time, and Electrolyte Concentration. ACS Applied Materials & Interfaces, 2012, 4, 6038-6045.	4.0	15
151	Nanoporous core–shell Cu@Cu2O nanocomposites with superior photocatalytic properties towards the degradation of methyl orange. RSC Advances, 2012, 2, 12636.	1.7	104
152	Preparation of mid-to-high molecular weight konjac glucomannan (MHKGM) using controllable enzyme-catalyzed degradation and investigation of MHKGM properties. Journal of Polymer Research, 2012, 19, 1.	1.2	8
153	Formation and microstructure of nanoporous silver by dealloying rapidly solidified Zn–Ag alloys. Electrochimica Acta, 2012, 63, 302-311.	2.6	72
154	Fabrication of bi-modal nanoporous bimetallic Pt–Au alloy with excellent electrocatalytic performance towards formic acid oxidation. Green Chemistry, 2011, 13, 1914.	4.6	49
155	Formation, control and functionalization of nanoporous silver through changing dealloying media and elemental doping. CrystEngComm, 2011, 13, 2617.	1.3	66
156	On the vacancy-controlled dealloying of rapidly solidified Mg–Ag alloys. CrystEngComm, 2011, 13, 4846.	1.3	10
157	Fabrication and characterization of magnetic nanoporous Cu/(Fe,Cu)3O4 composites with excellent electrical conductivity by one-step dealloying. Journal of Materials Chemistry, 2011, 21, 9716.	6.7	29
158	Novel nanocrystalline PdNi alloy catalyst for methanol and ethanol electro-oxidation in alkaline media. Journal of Power Sources, 2011, 196, 5823-5828.	4.0	180
159	Early-life history traits of two icefishes, spiny icefish Chaenodraco wilsoni and ocellated icefish Chionodraco rastrospinosus, in the Ross Sea revealed by otolith microstructure. Polar Biology, 0, , 1.	0.5	3